processes

MDPI

Article

Study on the Organic Geochemical Characteristics of Jurassic Source Rocks from the Northern Tibetan Plateau Basin

Yajun Shi, Li Xu *, Xinmin Ma and Jiajia Guo

Research Institute of Petroleum Exploration and Development Northwest, Petrol China, Lanzhou 730020, China
* Correspondence: xuli0055@petrochina.com.cn

Abstract

The Northern Tibetan Plateau Basin is the most extensive and least explored Mesozoic marine basin in China and shows considerable potential for oil and gas exploration. This study systematically analyzed the abundance, type, hydrocarbon generation potential, and conversion rate of organic matter within three Jurassic drill core samples from the Biloucuo area of the Northern Tibetan Plateau Basin. The total organic carbon (TOC) content of these Jurassic source rocks was >4%, on average, permitting their classification as excellent source rocks. The average contents of sapropelinite, exinite, vitrinite, and inertinite in kerogen were 74%, 4%, 18%, and 4%, respectively. The H/C and O/C ratios of the kerogen mainly ranged from 0.8 to 1.3 and 0.06 to 0.11, respectively, indicative of type II_1 kerogen. The average $S_1 + S_2$ content was 15.0 mg/g rock, indicating a high hydrocarbon generation potential. On the basis of the relationship between the quantity of soluble hydrocarbons remaining in the strata and the S_2 and TOC contents, it can be inferred that the hydrocarbon generation conversion rate of these Jurassic source rocks was between 25% and 50%, and partial hydrocarbon expulsion has taken place. It is estimated that the maximum oil generation potential of the formation will reach 20 kg/t rock at a greater depth, which equates to good exploration potential.

Keywords: The Northern Tibetan Plateau Basin; Jurassic; source rock; type and abundance of organic matter

Academic Editor: Dicho Stratiev

Received: 27 June 2025
Revised: 12 August 2025
Accepted: 20 August 2025
Published: 13 October 2025

Citation: Shi, Y.; Xu, L.; Ma, X.; Guo, J. Study on the Organic Geochemical Characteristics of Jurassic Source Rocks from the Northern Tibetan Plateau Basin. *Processes* **2025**, *13*, 3266. https://doi.org/10.3390/pr13103266

1. Introduction

According to the 73rd statistical review of World Energy [1], oil and gas resources are currently our largest global energy sources, and their consumption continues to increase. However, as oil and gas exploration become increasingly complicated, there is increasing pressure on production in better-explored fields and a need to discover new exploration areas to satisfy the increasing demand for oil and gas. The Northern Tibetan Plateau Basin is a large marine basin with relatively complete Mesozoic marine strata [2–4]. It shows excellent oil and gas resource potential [5,6], but has currently experienced a low degree of onshore oil and gas exploration. The Northern Tibetan Plateau Basin is located within the eastern section of the Tethys-Himalaya tectonic domain, which is known to contain substantial oil and gas resources; the domain comprises 17% of the world by area, but its oil and gas reserves account for two-thirds of the total global proven reserves [7,8]. The geological conditions of the Northern Tibetan Plateau Basin are similar to those of the adjacent western Middle East oil and gas area, and the southeast part of the Northern Tibetan Plateau Basin is Southeast Asia oil and gas. This particular tectonic setting and favorable geological conditions mean that petroleum investigation and exploration in

the Northern Tibetan Plateau Basin warrants further attention [3]. The Northern Tibetan Plateau Basin also has relatively complete Jurassic marine strata, including several sets of organic-rich shales. According to the overall situation of hydrocarbon source rocks in petroliferous basins, marine source rocks tend to have large distribution areas, a high abundance of organic matter, and high hydrocarbon generation potential. Hence, petroleum geologists have closely examined the characteristics of marine source rocks in the Northern Tibetan Plateau Basin.

In the late 1990s, a large-scale oil and gas survey was carried out in the Northern Tibetan Plateau Basin. More than 150 oil and gas sites were discovered, including one oil shale site [9–11]. Subsequently, several rounds of strategic selection, investigation, and evaluation of oil and gas resources have been carried out in the Tibetan exploration area, and a further three oil shale sites and several oil and gas sites have been discovered; this proves that the Northern Tibetan Plateau Basin possesses the primary conditions for oil and gas accumulation and has the potential for the development of commercial oil and gas fields. Although considerable investigation of the Northern Tibetan Plateau Basin has been carried out in recent years, the progress of exploration has been hampered by the harsh climate and topography of the Tibetan Plateau [12].

Oil and gas exploration best practices have shown that high-quality source rocks are a prerequisite for discovering medium- and large-scale oil and gas reservoirs in marine or continental basins. The material basis of oil and gas accumulation is high-quality source rocks with abundant organic matter, good type, and maturity in the oil generation window. However, previous research on source rocks in the Northern Tibetan Plateau Basin has mostly been based on outcrop samples and analysis over relatively scattered locations. The Tibetan Plateau experiences extreme weathering, which has a substantial impact on the geochemical characteristics of source rocks, especially the organic geochemical characteristics; this, in turn, has a substantial effect on the identification of source rocks and calculation of resource potential in the Northern Tibetan Plateau Basin [13–15]. Although previous studies have identified the presence of limestone-type source rocks in this area [16], research on the geochemical characteristics and hydrocarbon generation potential of these source rocks remains relatively underdeveloped. Therefore, it is vitally important to conduct geochemical analyses of drill core samples from the Northern Tibetan Plateau Basin to more accurately evaluate source rock characteristics and hydrocarbon generation potential. Taking three drill core samples from the Biloucuo area of the Northern Tibetan Plateau Basin as representative examples, this study systematically analyzes the geochemical characteristics of Jurassic source rocks and assesses their hydrocarbon generation potential. The data reported herein provide a reference for determining oil and gas resources and further exploration in the Northern Tibetan Plateau Basin.

2. Geological Setting

The Northern Tibetan Plateau Basin is a large Late Paleozoic-Mesozoic marine sedimentary basin [17]. Tectonically, the Northern Tibetan Plateau Basin is an important part of the large Tethys-Himalaya tectonic domain [16]. As shown in Figure 1, the Northern Tibetan Plateau Basin is bounded to the north by the Hoh Xil-Jinshajiang suture belt and to the south by the Bangong Hu-Nujiang suture belt [18–20] and can be divided into three structural units from north to south: north depression, central uplift belt, and south depression [19,20]. The Biloucuo area studied herein is located in the Shuanghu area of the south depression.

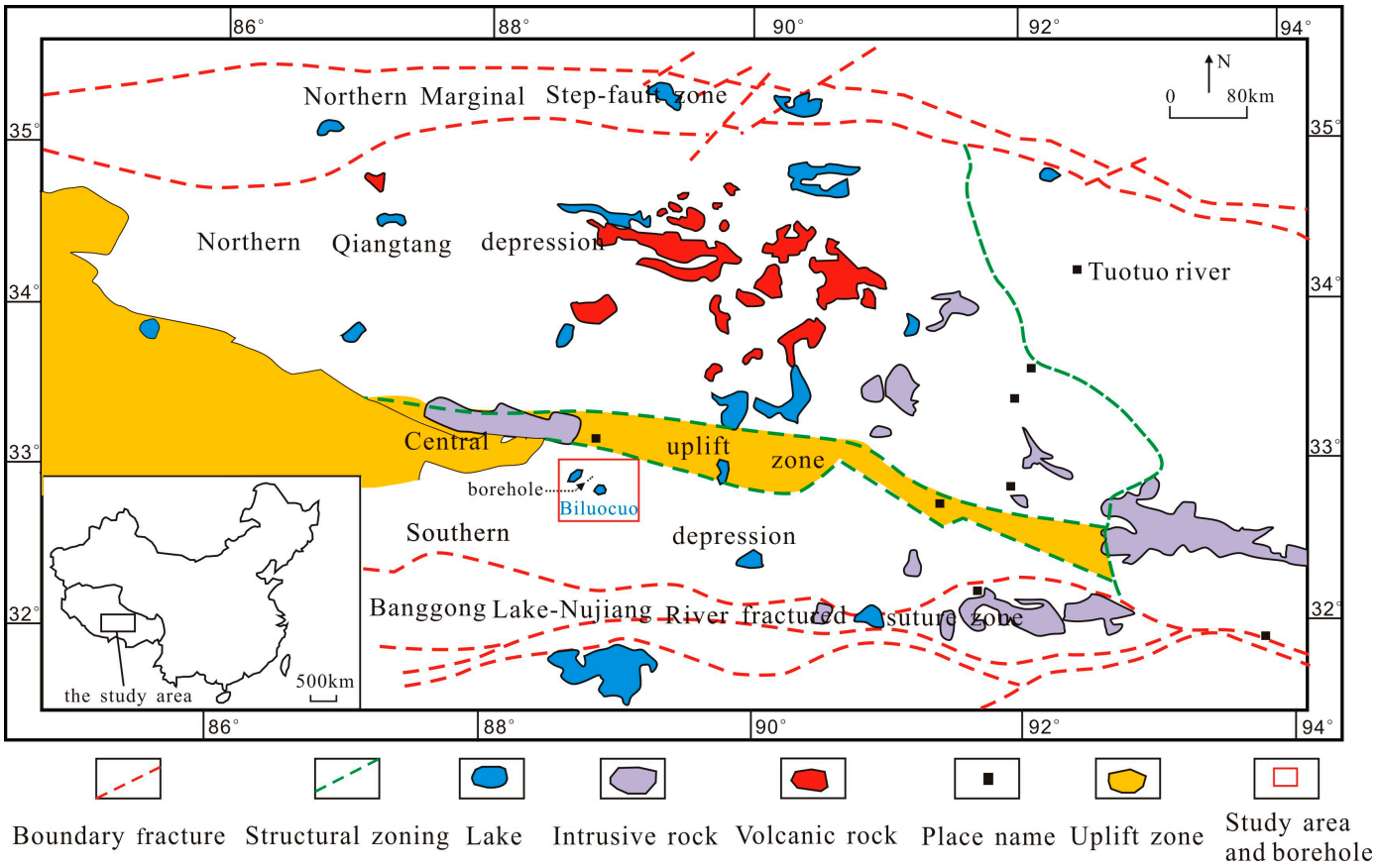

Figure 1. Geographical location and structural characteristics of the Northern Tibetan Plateau Basin (Modified according to Reference [6]).

The present emergent strata in the Northern Tibetan Plateau Basin are of the Triassic, Jurassic, and Cretaceous age. The Jurassic marine strata are (from bottom to top): Lower Jurassic Quse Formation (J_1q), Lower-Middle Jurassic Quemoco Formation ($J_{1-2}q$), Middle Jurassic Buqu (J_2b) and Xiali (J_2x) Formations, Upper Jurassic Sowa Formation (J_3s), and Upper Jurassic-Lower Cretaceous Bailongice Formation (J_3s) [12,16]. Among these, the Middle and Upper Jurassic is characterized by the mutual association of different strata, including the Jiabuqu clastic rocks and Sowa limestone of the Quemoco, Xiali, and Xueshan formations. Overall, the thickness of the Jurassic strata is >3000 m, and the thickness of the Lower Jurassic Quse Formation shale is >100 m (Figure 2). Among them, the Xiali (J_2x) of the Middle Jurassic was formed as a reservoir, and its lithological characteristics were mainly lithic quartz sandstone.

The Baqu formation was formed as the basin underwent large-scale marine transgression, during which great thicknesses of marine platform carbonates were deposited. These carbonates include micrite, organic limestone, bioclastic limestone, and marl [16].

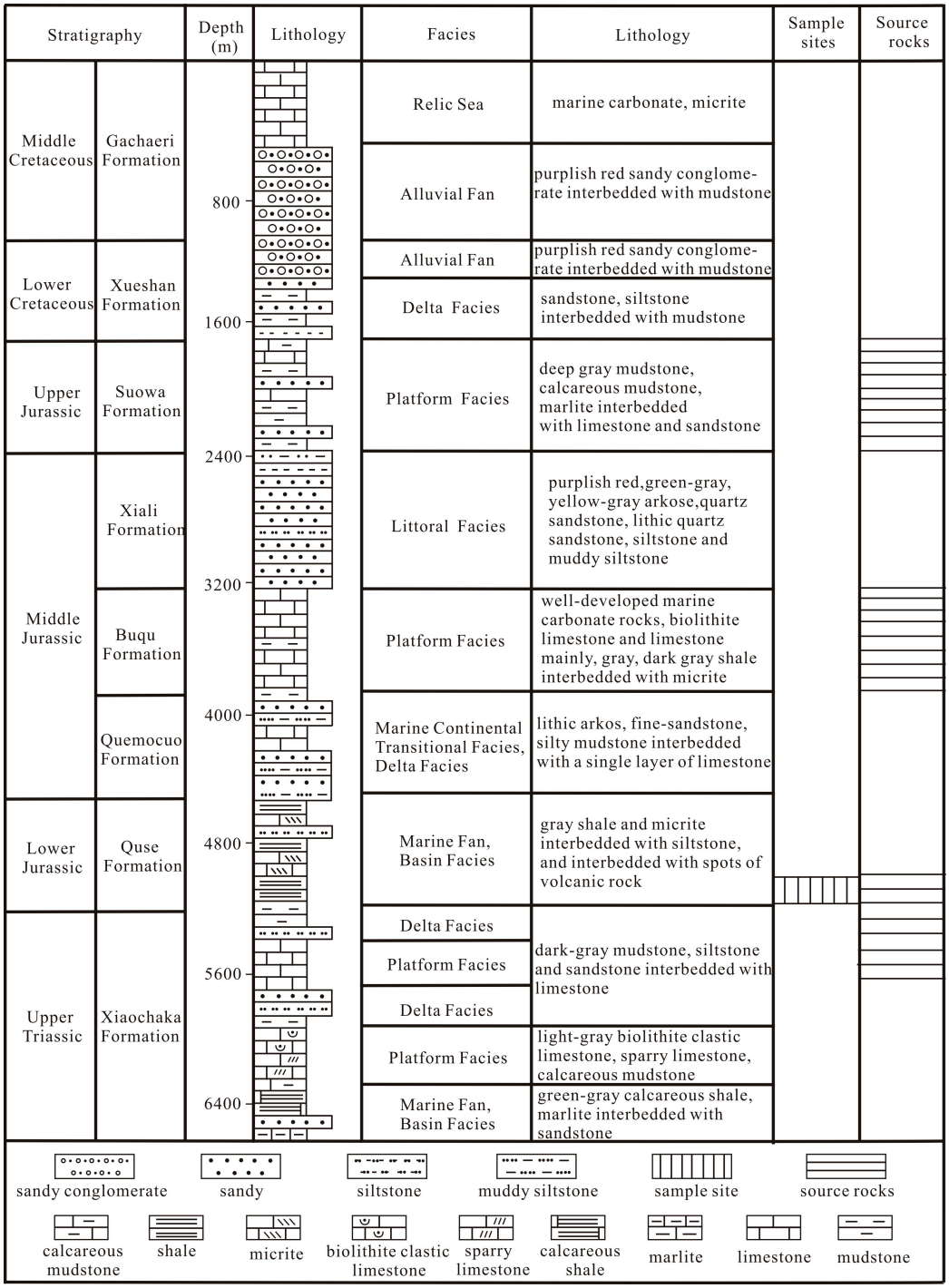

Figure 2. Development characteristics of strata and lithology in the Northern Tibetan Plateau Basin [12].

3. Samples and Methods

3.1. Samples

Source rock samples in this study were mainly retrieved from wells BK1, BK2, and BK3 in the Biloucuo area of the Northern Tibetan Plateau Basin. The drill cores were from shallow wells with drilling depths of <200 m, and the lithology was mainly marly limestone. A total of 88 source rocks were collected, including 29 from BK1, 22 from BK2, and 37 from BK3. The depths of drill core samples ranged from 2.6 m to 116.7 m, 2.4 m to 127.9 m, and 3.7 m to 117.1 m in wells BK1, BK2, and BK3, respectively, with an average interval of approximately 4 m. Total organic carbon (TOC) content, rock pyrolysis, and

chloroform asphalt "A" analyses were performed on all samples. Kerogen separation, maceral identification, and elemental composition analysis of source rock samples were also carried out.

3.2. Methods

The collected drill core source rock samples were first cleaned to remove surface dust or paint. The samples were then crushed to 100 mesh; approximately 100 mg of each sample was placed in a crucible, and 3% hydrochloric acid was slowly added (drop by drop) to remove the carbonate. When the sample was no longer bubbling, the crucible was filled with diluted hydrochloric acid and boiled at 80 °C for 4 h. Finally, the chloride ions in the sample and crucible were removed using deionized water, and the sample was dried. The TOC content was measured using a CSI analyzer, and pyrolytic analysis was performed using a Rock-eval 6 pyrolysis analyzer.

The analysis method for soluble hydrocarbons in the source rock samples was as follows: each drill core sample was crushed to 100 mesh and extracted via the Soxhlet method using a mixture of methylene chloride:methanol (93:7, *v*:*v*) for 72 h to obtain chloroform asphalt "A". After the asphaltene in asphalt "A" of chloroform was precipitated with *n*-hexane, column chromatography was used to separate the saturated hydrocarbons, aromatic hydrocarbons, and non-hydrocarbons using *n*-hexane, *n*-hexane:dichloromethane (1:2, *v*:*v*), and methanol, respectively. The saturated hydrocarbon fractions were analyzed and identified by gas chromatography–mass spectrometry (GC-MS) using an Agilent Technologies Inc. instrument. The parameters were as follows: MS of 5973N, ion source temperature of 250 °C, and ionizing voltage of 70 eV. GC was 6890N, the chromatographic column was HP-5MS (30 m × 0.25 mm), the film thickness of the fixed phase was 0.25 μm, the carrier gas was high-purity helium, the initial temperature was 80 °C, the temperature was increased to 290 °C at 4 °C/min, and then the temperature was maintained at a constant for 30 min.

The samples selected in this study were mainly oil shales and marlstone. To separate kerogen from each drill core sample, the sample was first roughed to approximately 0.5 mm, fully leached with hydrochloric and hydrofluoric acid, and then heated with 10% HCl for approximately 2 h (at 80 °C). After cessation of the reaction, the acid solution was centrifuged, drained away, and then washed to neutral with deionized water to thoroughly remove calcium ions in the sample. Subsequently, HCl (10%) and HF (10%) of twice the volume were added, heated at 80 °C, and stirred continuously for 2 h to remove silicates from the sample. Finally, the acid solution was emptied and washed in deionized water until neutral. The acid-treated kerogen was subjected to flotation with a 2.0 g/mL specific gravity solution (HI + KI + Zn), and the flotation products were prepared as slides. The organic matter components and types of microfossils were identified and counted using transmitted light and fluorescence under a binocular biological microscope. After the remaining sample was dried, the elemental content (C, H, O, N, and S) of the kerogen was detected using an EA1110 elemental analyzer.

4. Results and Discussion

4.1. Organic Matter Abundance and Soluble Hydrocarbon Composition of Source Rocks

The TOC contents of the Jurassic drill core samples from wells BK1, BK2, and BK3 in the Biloucuo area ranged from 0.48% to 17.40%, 0.49% to 16.60%, and 0.40% to 20.70%, respectively, with average values of 4.42%, 4.80%, and 4.04%, respectively (Figures 3–5). These very high organic matter abundances indicate that the Jurassic rocks in this area are good source rocks with a high exploration potential. Mud shale with a TOC content >0.5% is considered an effective source rock, while a TOC content >2% is regarded as a

very high-quality source rock [21,22]. Nearly all the samples analyzed from this study area had TOC contents >0.5%. Samples with TOC contents >2% accounted for 48.3% (14/29), 54.5% (12/22), and 70.3% (26/37) of the selected BK1, BK2, and BK3 samples, respectively. These data indicate that each drill core comprised >100 m of potential source rocks, and over half of the samples could be classified as high-quality source rocks.

The soluble hydrocarbon content (chloroform asphalt "A") in present-day geological samples is another critical parameter for evaluating the abundance of organic matter in source rocks. The content of bitumen "A" in Jurassic drill core samples from wells BK1, BK2, and BK3 ranged from 0.2 to 9.8, 0.1 to 7.0, and 0.2 to 17.6 mg/g of rock, respectively, with average values of 2.9, 2.8, and 3.4 mg/g of rock, respectively. In terms of the soluble hydrocarbon group composition, the average content of saturated hydrocarbons in bitumen "A" of wells BK1, BK2, and BK3 was 27.6%, 31.7%, and 44.5%, respectively, and the average content of aromatic hydrocarbons was 14.2%, 15.7%, and 16.0%, respectively. The combined proportion of saturated and aromatic hydrocarbons was between 40% and 60%, and the total hydrocarbon content accounted for approximately half of the total chloroform asphalt "A" content. Previous studies have proposed that shale with a total hydrocarbon content >200 ppm (0.2 mg/g of rock) can be regarded as an effective source rock, and shale with a total hydrocarbon content >1000 ppm (1.0 mg/g of rock) can be considered a very high-quality source rock [22]. In our study, 51.7% (15/29), 45.5% (10/22), and 62% (23/37) of the samples from wells BK1, BK2, and BK3, respectively, had chloroform asphalt "A" contents >2.0 mg/g of rock.

From the above results, the proportions of effective source rocks and high-quality source rocks according to their chloroform asphalt "A" or total hydrocarbon contents is slightly lower than those according to their TOC contents. This may be explained in two ways. First, although shallow drill core samples were used in this study, chloroform asphalt "A" may have suffered slight losses, while TOC, mainly comprising the carbon content of solid kerogen, was less affected. Second, the Jurassic source rocks in this study have a high TOC content, and such organic-rich source rocks tend to have a higher oil discharge efficiency. Hence, some soluble hydrocarbons may have been discharged from the source rocks with the passing of geological time. The chloroform asphalt "A" and total hydrocarbon contents measured at present represent the number of residual hydrocarbons, so their contents may be somewhat reduced.

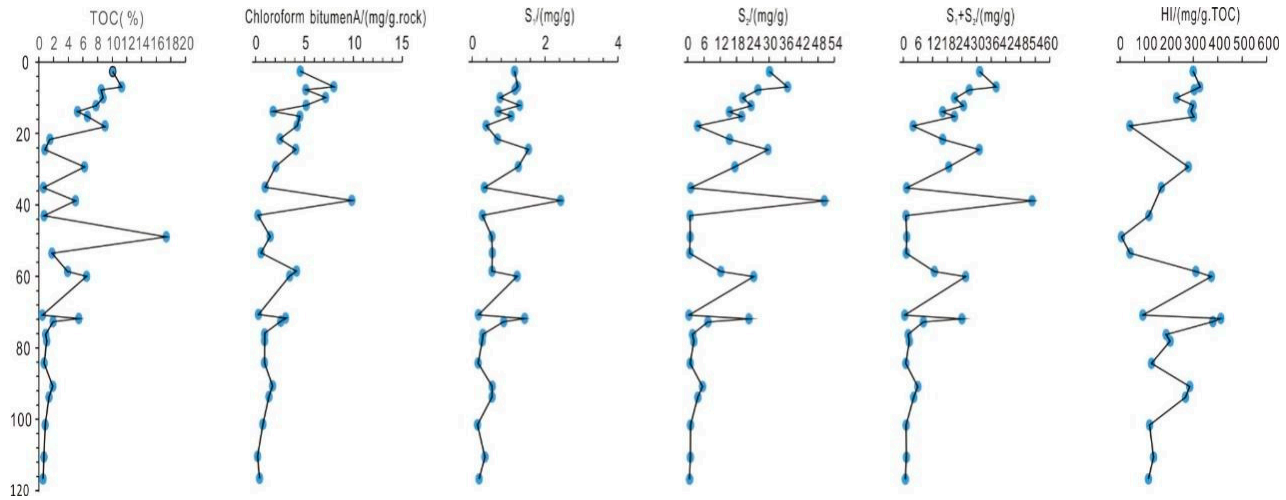

Figure 3. Composite profiles of well BK1.

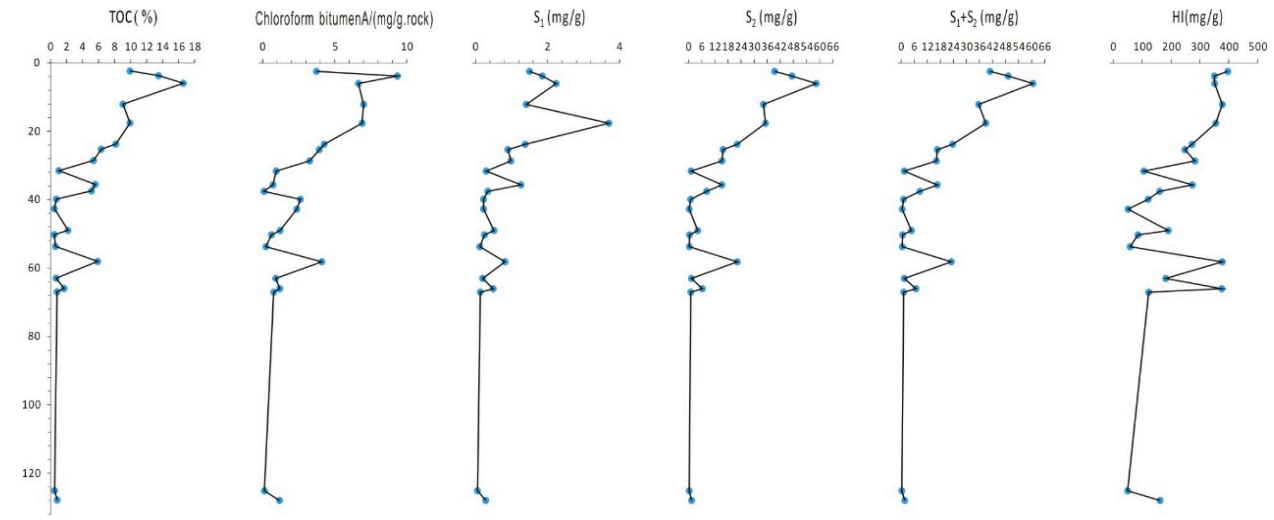

Figure 4. Composite profiles of well BK2.

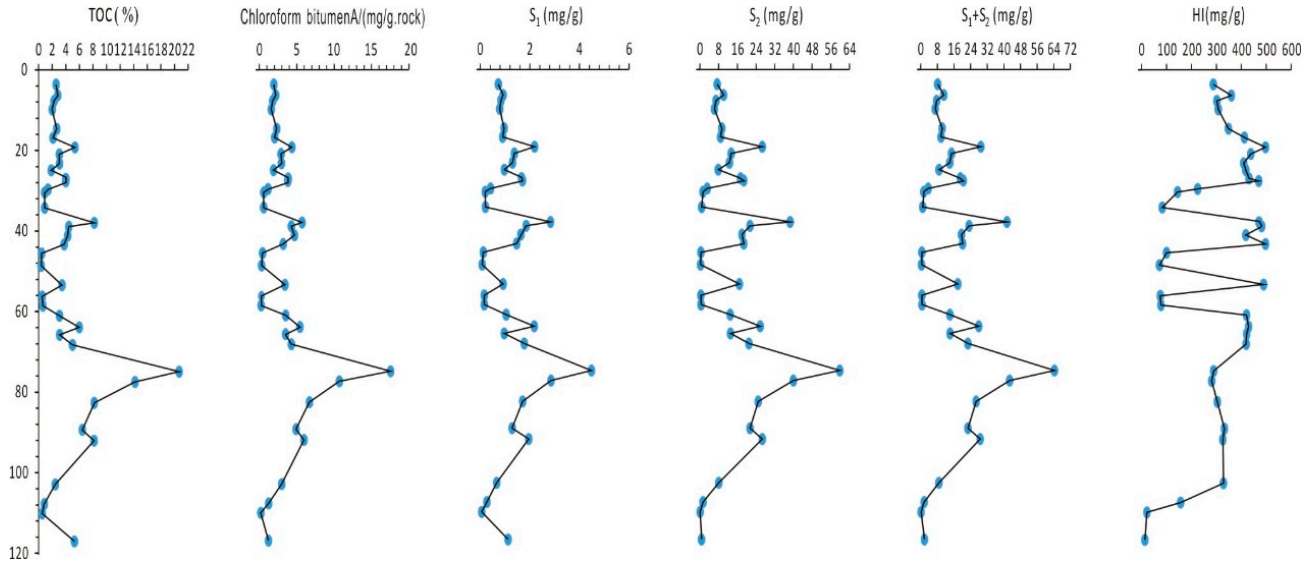

Figure 5. Composite profiles of well BK3.

4.2. Types of Organic Matter in the Jurassic Source Rocks

The type of organic matter usually reflects the hydrocarbon generation characteristics of a source rock [23]. Standard methods used to classify types of organic matter in source rocks include rock pyrolysis, kerogen microscopy, and atomic ratios. Previous studies have shown that the organic matter in source rocks of the Northern Tibetan Basin is complex, and includes type I, type II, and type III; for Jurassic source rocks, types I and II_1 are dominant, with small amounts of type II_2 [24,25]. The results of the sample pyrolysis herein showed that the hydrogen index (HI) of Jurassic source rocks in the Biloucuo area of the Northern Tibetan Basin was mainly between 100 and 500 mg/g TOC, and the organic matter was mainly of the type II variety, with >60% of samples being of type II_1 (Figure 6a). The elemental analysis of kerogen showed that the H/C and O/C ratios of samples mainly ranged from 0.8 to 1.3 and 0.06 to 0.11, respectively (Figure 6b). According to kerogen atomic ratio classification, both of these ranges of ratios equate to type II_1 organic matter (Figure 6b), giving somewhat different results to those using the HI division.

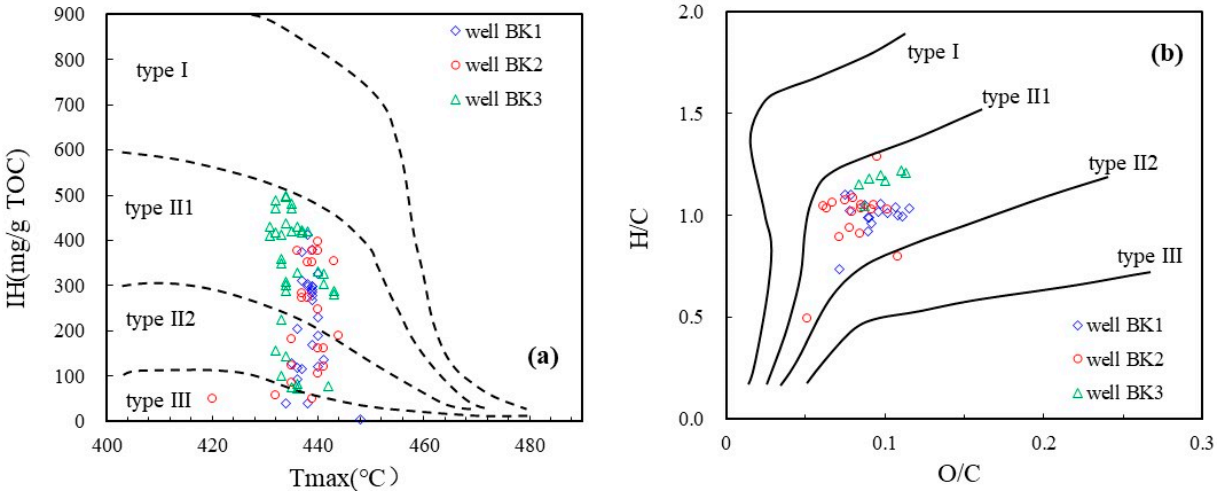

Figure 6. Classification maps of Jurassic source rock organic matter in the Biloucuo area of the Northern Tibetan Basin ((**a**): The intersection graph between T_{max} and IH. (**b**): The intersection graph between O/C and H/C.).

Microscopic examination of kerogen macerals is regarded as the most direct method for classifying types of organic matter [26]. The average contents of sapropelinite, exinite, vitrinite, and inertinite in kerogen samples in this study were 74%, 4%, 18%, and 4% (Figure 7), respectively. Therefore, the maceral components of Jurassic source rocks in the Biloucuo area are evidently mainly sapropelinite with a small amount of vitrinite, while the contents of exinite and inertinite are relatively minor. It is generally believed that the sapropel group is mainly formed by the remains of lower aquatic plants, phytoplankton, algae and some zooplankton through sapropelization, which is formed in a stagnant anaerobic environment. The kerogen type index (TI) values calculated according to the maceral content indicate that all analyzed samples belong to type II_1 organic matter (Table 1), consistent with the results obtained using kerogen atomic ratios. It shows that the organic matter type of the sample is better.

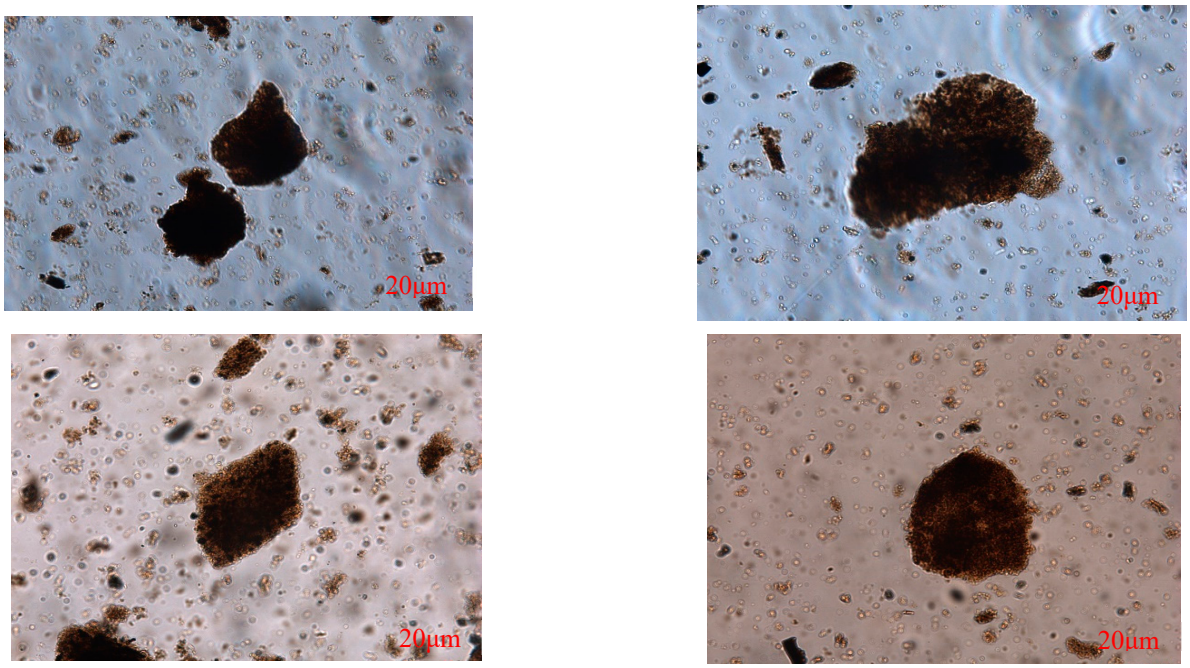

Figure 7. Micrographs of kerogen of Jurassic source rock organic matter in the Biloucuo area of the Northern Tibetan Basin.

Table 1. Kerogen maceral composition for the BK1, BK2, and BK3 source rock samples from the Biloucuo area of the Northern Tibetan Basin.

Well	Depth	Sapropelic	Exinite	Vitrinite	Inertinite	TI	Kerogen Type
	(m)	(%)	(%)	(%)	(%)		
BK1	2.6	52.50	5.00	37.50	5.00	21.88	II2
BK1	6.94	49.53	3.74	43.30	3.43	15.50	II2
BK1	7.78	65.56	5.30	22.85	6.29	44.78	II1
BK1	9.98	70.07	3.62	23.03	3.29	51.32	II1
BK1	12.17	74.36	3.21	18.91	3.53	58.25	II1
BK1	13.86	69.06	3.75	22.19	5.00	49.30	II1
BK1	15.21	85.48	1.65	9.57	3.30	75.83	II1
BK1	17.87	84.49	3.30	8.58	3.63	76.07	II1
BK1	21.58	83.12	2.55	10.51	3.82	72.69	II1
BK1	24.5	76.40	4.97	12.73	5.90	63.43	II1
BK1	29.3	77.22	3.48	16.14	3.16	63.69	II1
BK1	38.8	55.78	4.29	33.66	6.27	26.40	II2
BK1	48.9	64.41	4.71	26.18	4.71	42.43	II1
BK1	58.6	69.06	5.63	21.56	3.75	51.95	II1
BK1	60	69.75	3.82	22.93	3.50	50.96	II1
BK1	71.8	71.79	3.13	20.06	5.02	53.29	II1
BK2	2.4	72.93	5.10	18.79	3.18	58.20	II1
BK2	3.77	75.74	3.61	14.43	6.23	60.49	II1
BK2	5.98	75.66	2.96	16.12	5.26	59.79	II1
BK2	12.1	82.84	4.95	8.58	3.63	75.25	II1
BK2	17.6	74.37	4.11	15.51	6.01	58.78	II1
BK2	23.75	71.43	3.25	19.16	6.17	52.52	II1
BK2	25.3	65.71	5.13	22.76	6.41	44.79	II1
BK2	28.6	76.80	5.33	12.85	5.02	64.81	II1
BK2	31.56	79.10	2.89	12.22	5.79	65.59	II1
BK2	35.6	76.87	5.21	14.66	3.26	65.23	II1
BK2	37.5	77.04	5.35	12.26	5.35	65.17	II1
BK2	39.86	76.60	6.41	12.82	4.17	66.03	II1
BK2	42.7	65.47	3.58	25.73	5.21	42.75	II1
BK2	49	82.32	2.57	10.93	4.18	71.22	II1
BK2	50.25	64.72	5.18	23.95	6.15	43.20	II1
BK2	53.7	73.86	3.27	16.01	6.86	56.62	II1
BK2	58.1	81.96	4.11	9.81	4.11	72.55	II1
BK3	3.7	78.10	5.23	13.07	3.59	67.32	II1
BK3	7.8	81.37	6.54	8.50	3.59	74.67	II1
BK3	14.7	75.39	5.68	15.46	3.47	63.17	II1
BK3	19.3	77.33	5.90	12.11	4.66	66.54	II1
BK3	23.3	80.92	3.95	11.84	3.29	70.72	II1
BK3	27.1	78.39	2.90	16.13	2.58	65.16	II1
BK3	30.5	67.54	2.62	24.59	5.25	45.16	II1
BK3	34.3	71.80	6.23	16.72	5.25	57.13	II1
BK3	38	72.67	5.79	17.36	4.18	58.36	II1
BK3	43.4	73.33	4.76	19.37	2.54	58.65	II1
BK3	53.5	83.60	3.15	11.36	1.89	74.76	II1
BK3	58.6	85.29	1.96	9.80	2.94	75.98	II1
BK3	61.1	41.80	5.14	51.13	1.93	4.10	II2
BK3	65.8	76.03	4.73	16.09	3.15	63.17	II1
BK3	68.3	83.12	1.91	12.42	2.55	72.21	II1

Some samples were classified as type II_2 organic matter in the T_{max}-HI chart; in contrast, using kerogen atomic ratios or microscopic examination, these samples were classified as type II_1 organic matter. This difference may be caused by the calculation of HI being dependent on the potential of S_2 in rock pyrolysis analysis, which contains a fraction of the components of chloroform asphalt "A". Compared with kerogen, these soluble hydrocarbons are more susceptible to late modification [27]. Therefore, when the soluble hydrocarbon content is affected, the content of pyrolysis parameter S_2 will also be affected, ultimately resulting in a lower rock HI.

4.3. Characteristics of Organic Matter Sedimentary Environment and Biomarker Compounds from Biological Sources

(1) Organic matter sedimentary environment

The ratio of Pr/Ph in the Biloucuo area of the Northern Tibetan Basin ranges from 0.47 to 0.71, with a mean value of 0.56 (Figure 8). The distribution of Pr/Ph in the crude oil samples is concentrated, showing a strong phytane advantage [28–30]. The Pr/nC_{17} and Ph/nC_{18} values of the samples in the study area are mainly distributed between 0.12~1.80 and 0.21~3.75, respectively. The Pr/nC_{17} and Ph/nC_{18} values of the source samples are narrowly distributed (Figure 9), indicating their origin from a similar biological source. The samples are mainly distributed in the strongly reducing marine environment with type I and type II organic matter as the parent material.

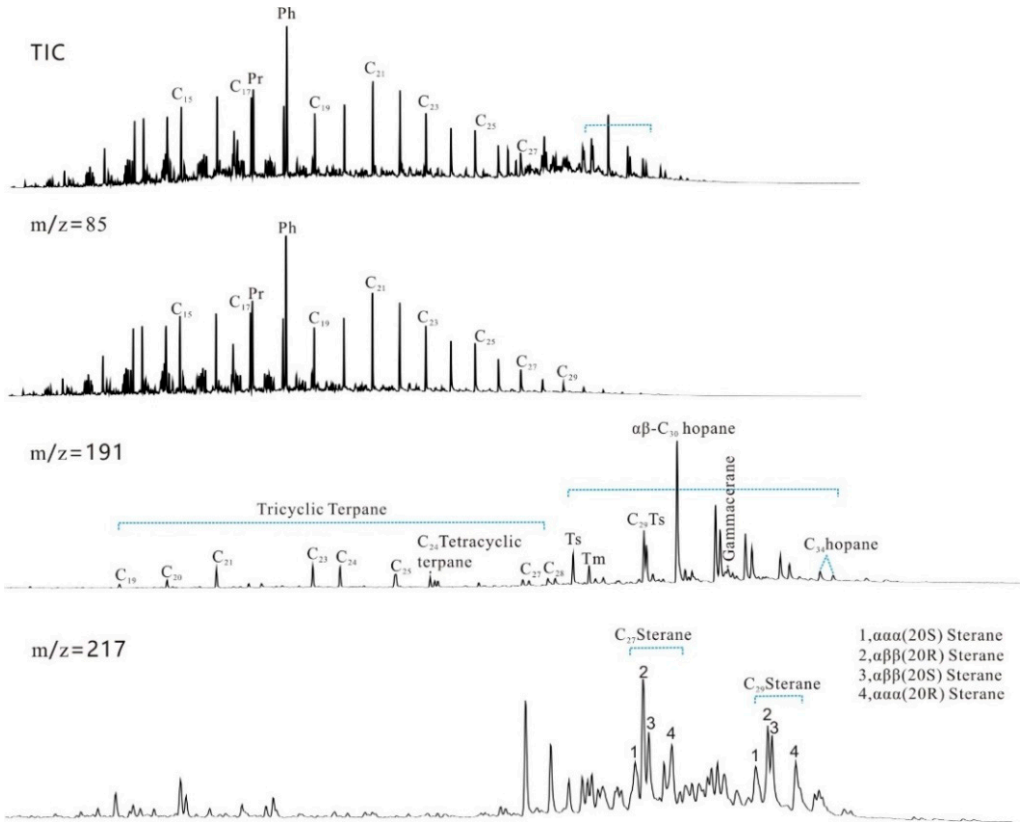

Figure 8. Total ion current, *m*/*z*85, *m*/*z*191, and *m*/*z*217 fragmentograms of saturated fractions of source rock in the Biloucuo area of the Northern Tibetan Basin.

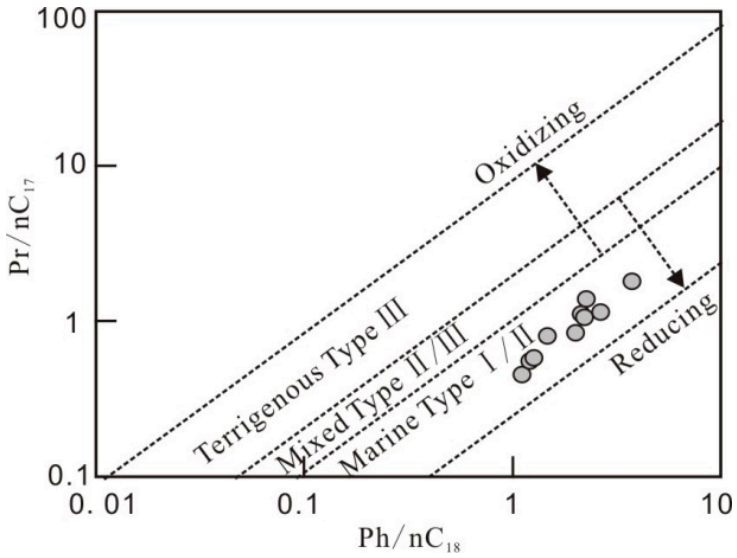

Figure 9. Plots of Pr/nC_{17} vs. Ph/nC_{18} ratios of source rock in the Biloucuo area of the Northern Tibetan Basin.

The relative content of gammacerane is positively correlated with paleosalinity [31,32], which is an important indicator of water salinity. The relative content of C_{34} + C_{35} homohopane ranges from 2% to 10%, and the average is 4%, and a distinct, not obvious tail-warping phenomenon is visible in the high carbon number region of hopane. The gammcerane/αβ-C_{30} hopane in the study's source samples ranges from 0.06 to 0.14 (average 0.08); the value is lower than the ratio of gammcerane/αβ-C_{30} hopane in source rocks of salt lake origins, such as the gammcerane/αβ-C_{30} hopane ratio of 0.27~1.0 in source rocks of salt lake origins in the western Qaidam Basin, and higher than that of freshwater origin, such as the gammcerane/αβ-C_{30} hopane ratio of 0.04~0.06 in source rocks of freshwater origins in Xifeng Olifield, Ordos.

All of the above indicators justify that the crude oil was formed in a low-salt sedimentary environment [33], and others have detected a certain content of gammacerane in crude oil samples from various oil seeps in the Tibetan Basin. However, its abundance is relatively low. The study suggests that the crude oil originated from a bay estuary environment with significant freshwater input or an open sea environment. This further proves that this set of low-salinity source rocks are the hydrocarbon-supplying source rocks for the Northern Tibetan Basin.

(2) Organic matter biological sources

The distribution characteristics of *n*-alkanes in source rocks can be used to identify the parental material of crude oil formation [23,32]. The source rocks of the Biloucuo area in the Northern Tibetan Basin possess similar *n*-alkane distribution characteristics. The carbon number distribution ranges from C_{12} to C_{37}. The distribution is a bimodal peak, where the forward peak carbon number is C_{17} and post peak carbon number is C_{21}. Mixed carbon number *n*-alkanes are the dominant fraction, reflecting that the input of the source rocks' parent material is mainly composed of aquatic organisms but is also contributed to by terrestrial higher plants.

In general, C_{29} sterols are the main cholesterol type in higher plants, whereas aquatic algae contain comparatively high C_{27} sterol levels. Sterane originates from sterols [34,35], and, therefore, the relative abundance of $C_{27}ααα$(20R) sterane, $C_{28}ααα$(20R) steranes, and $C_{29}ααα$(20R) steranes in samples can be used to reflect the source of the organic matter of the parent material. The $C_{27}ααα$(20R) sterane content in the source rocks in the study area ranges from 36% to 75%, with an average of 45%, while the $C_{29}ααα$(20R) sterane content

ranges from 16% to 46%, with an average of 39% (Figure 10, Table 2). The samples indicate the predominance of $C_{27}\alpha\alpha\alpha$(20R), which shows that the parent material of the samples is mainly derived from aquatic algae but also contributed to by terrestrial higher plants.

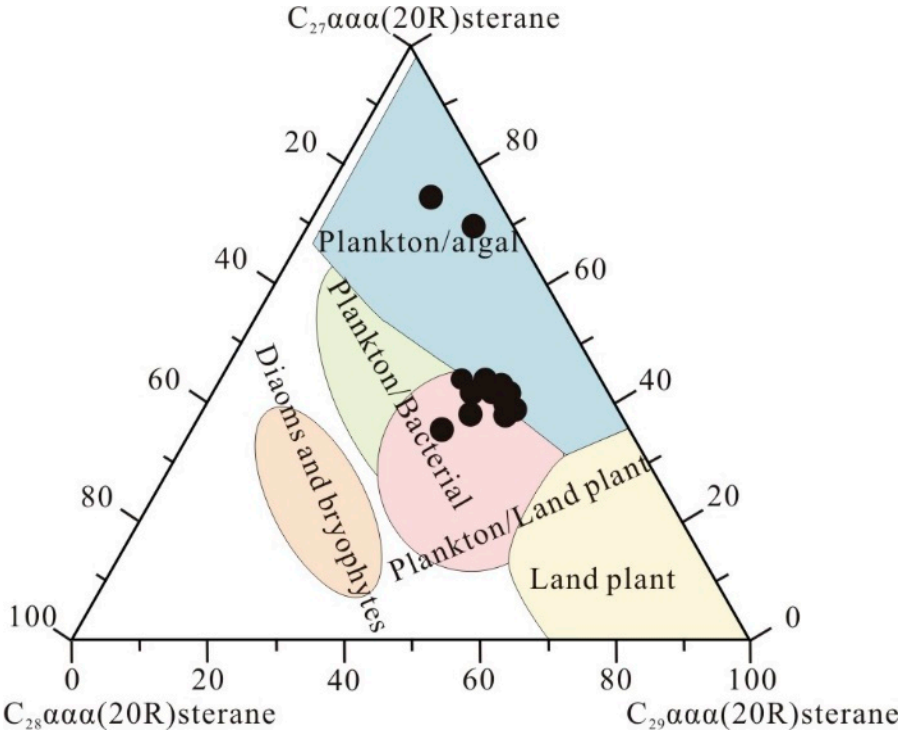

Figure 10. Ternary plot of $C_{27}\alpha\alpha\alpha$(20R), $C_{28}\alpha\alpha\alpha$(20R), and $C_{29}\alpha\alpha\alpha$(20R) sterane of source rock in the Biloucuo area of the Northern Tibetan Basin (according to reference [33]).

Table 2. Selected sterane indices for the oil samples and source rock samples.

	Depth (m)	1	2	3	4	5	6	7	8
Source rock samples from BK3	5.6	38	22	39	0.45	0.63	0.38	0.16	1.03
	7.9	42	16	42	0.45	0.62	0.39	0.15	0.99
	10.1	43	15	41	0.45	0.63	0.40	0.14	0.95
	15.3	42	15	43	0.45	0.63	0.38	0.15	1.02
	19.5	39	15	46	0.46	0.62	0.35	0.17	1.18
	25.1	40	16	43	0.45	0.61	0.38	0.18	1.08
	27.6	38	17	45	0.45	0.62	0.33	0.18	1.19
	33.0	40	16	44	0.46	0.60	0.35	0.18	1.11
	35.2	40	16	44	0.47	0.62	0.33	0.16	1.09
	53.2	44	17	39	0.48	0.60	0.38	0.14	0.88
	57.4	70	5	25	0.47	0.68	0.98	0.11	0.36
	60.0	42	17	41	0.46	0.61	0.40	0.16	0.98
	65.5	36	28	37	0.49	0.61	0.28	0.15	1.02
	69.8	42	20	38	0.39	0.64	0.40	0.14	0.92
	73.1	75	9	16	0.53	0.62	0.81	0.06	0.22

1: The relative content of $C_{27}\alpha\alpha\alpha$(20R) sterane; 2: the relative content of $C_{28}\alpha\alpha\alpha$(20R) sterane; 3: the relative content of $C_{29}\alpha\alpha\alpha$(20R) sterane; 4: $C_{29}\alpha\alpha\alpha$(20S)/(20S + 20R) sterane; 5: $C_{29}\beta\beta/(\beta\beta + \alpha\alpha)$ sterane; 6: $C_{27}\alpha\alpha\alpha$(20R)/C_{28} sterane; 7: $C_{29}\alpha\alpha\alpha$(20R)/C_{27} sterane; and 8: $C_{29}\alpha\alpha\alpha$(20R)/C_{27} $\alpha\alpha\alpha$(20R) sterane.

4.4. Evaluation of Hydrocarbon Generation Potential of Jurassic Source Rocks

The most common parameters used to evaluate the hydrocarbon generation potential of source rocks are S_1 and S_2; S_1 is associated with the soluble hydrocarbon content, and S_2 represents hydrocarbons generated via pyrolysis [20,36]. The results of the pyrolysis analysis in this study showed that the $S_1 + S_2$ contents of Jurassic drill core samples from wells BK1, BK2, and BK3 ranged from 0.6 to 52.8, 0.3 to 49.2, and 0.2 to 64.4 mg/g of rock, respectively, with average values of 13.7, 15.9, and 15.3 mg/g of rock, respectively. This indicates that the hydrocarbon generation potential of Jurassic source rocks in this area is very high. As can be seen from Figure 11a, in well BK1, there was no apparent relationship between the TOC content and hydrocarbon generation potential ($S_1 + S_2$), while these parameters showed good linear relationships in wells BK2 and BK3. Generally, when organic matter is evenly distributed and no large-scale hydrocarbon migration occurs, $S_1 + S_2$ correlate well with the TOC content. If there is no significant correlation between these parameters in a well, this indicates that some differentiation of organic matter type or hydrocarbon migration has occurred (affecting the value of S_1). There was no apparent correlation between the soluble hydrocarbon and TOC contents in well BK1, while good linear relationships occurred between these parameters in wells BK2 and BK3 (Figure 11b). As can be seen from Figure 6, the HI and H/C of well BK1 were lower than those of wells BK2 and BK3. One possible explanation for this is that the organic matter type within well BK1 is worse than that within wells BK2 and BK3. Alternatively, the maturity of well BK1 may be slightly higher than that of wells BK2 and BK3, reducing the hydrocarbon generation potential of the former. An increase in maturity leads to the light component of the product, which is more likely to result in hydrocarbon migration.

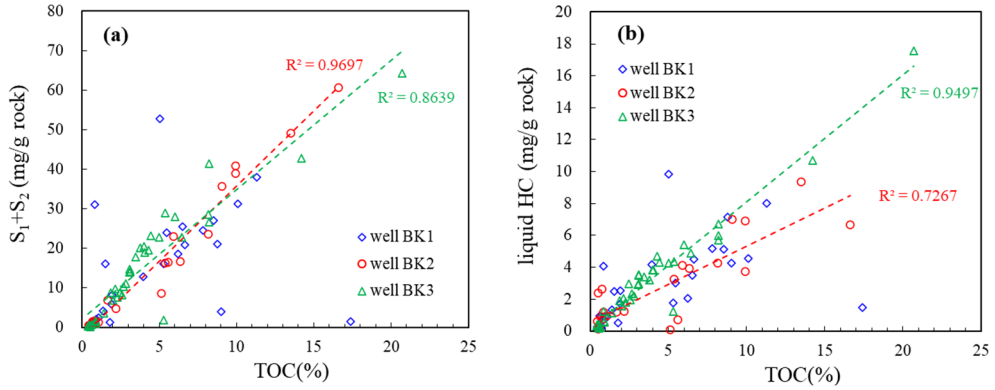

Figure 11. Relationships between (**a**) TOC content and hydrocarbon generation potential and (**b**) TOC content and soluble hydrocarbon content of source rocks.

Figure 12 shows the correlations between S_2 and soluble hydrocarbons under the conditions of a 25%, 50%, and 100% hydrocarbon generation conversion rate of typical type II_1 source rocks (initial HI value is 600 mg/g TOC), without considering hydrocarbon expulsion. It can be seen that S_2 substantially decreases, while soluble hydrocarbons gradually increase with an increase in the hydrocarbon generation conversion rate. The soluble hydrocarbon contents of drill core samples in the Biloucuo area have a good correlation with S_2 (Figure 12a). From this perspective, there is no noticeable difference in the organic matter properties of BK1, BK2, and BK3; hence, the differences observed in Figure 7 may be a result of hydrocarbon expulsion. In addition, Figure 11 also indicates that the hydrocarbon generation conversion rate in the Jurassic source rocks of the Biloucuo area is approximately 25%. However, it should be noted that this does not consider the condition of hydrocarbon expulsion.

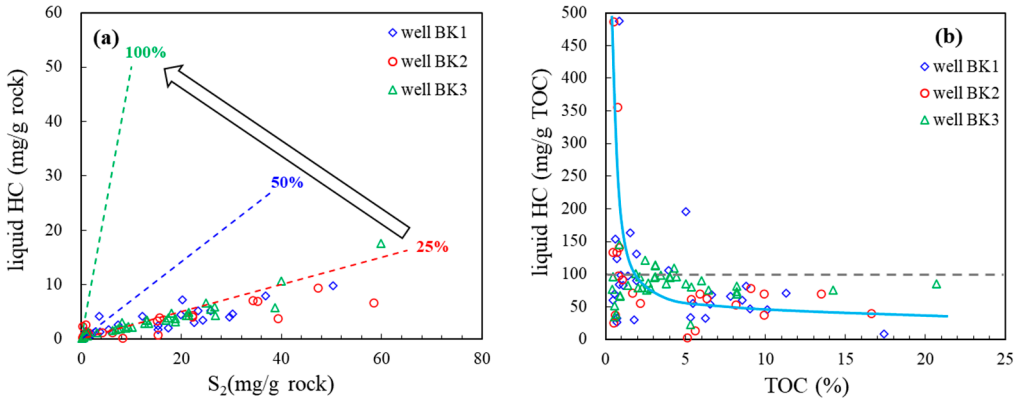

Figure 12. Hydrocarbon generation conversion rate and soluble hydrocarbon content per unit TOC of Jurassic source rocks in the Biloucuo area of the Northern Tibetan Basin ((**a**): The intersection graph of parameters S_2 and liquid HC. (**b**): The intersection graph of parameters TOC and liquid HC.).

All the soluble hydrocarbons present in the source rocks today are residual after hydrocarbon expulsion. In other words, 25% is the minimum conversion rate of the Jurassic source rocks in the Biloucuo area. If half of the generated hydrocarbons have subsequently been discharged, the conversion rate is 50%. Notably, when source rocks have similar types of organic matter and a similar maturity, the amount of soluble hydrocarbons (mg/gTOC) under a given TOC condition should be similar. As shown in Figure 12b, the amount of soluble hydrocarbons per unit TOC differs and gradually decreases with an increase in TOC content. This also indicates that a partial hydrocarbon expulsion has occurred in the Jurassic source rocks of the Biloucuo area, which is consistent with the fact that several oil shoots have been discovered.

Overall, no matter the oil discharge efficiency of the source rocks, the conclusion that Jurassic source rocks in the Biloucuo area have a high hydrocarbon generation potential is beyond doubt. It is estimated that the average TOC content of Jurassic source rocks in the Biloucuo area at a depth of approximately 110 m is 4% based on the oil generation capacity of typical type II_1 marine source rocks of approximately 500 mg/gTOC; this indicates that the maximum oil generation capacity of the source rocks may reach 20 kg/t of rock. Previous studies have shown that the maximum burial depth of Jurassic source rocks in the Northern Tibetan Basin is 5000–6000 m, and the corresponding thermal maturity is 1.1%–1.3% [37]; this indicates that in the depositional center, or in areas with a greater burial depth, the Biloucuo source rocks have reached the peak of oil generation and have particularly high potential soluble hydrocarbon and oil discharge efficiency, and, therefore, good exploration potential.

5. Conclusions

The Jurassic strata in the Biloucuo area of the Northern Tibetan Basin have developed multiple sets of marine carbonate source rocks primarily composed of marly limestones. These are source rocks with hydrocarbon generation potential, and the limestone is a more favorable source rock than the mudstone.

The average TOC content of Jurassic source rocks in the Biloucuo area of the Northern Tibetan Basin was >4%, which equates to an excellent-quality source rock. In kerogen, the average contents of sapropelinite, exinite, vitrinite, and inertinite were 74%, 4%, 18%, and 4%, respectively. The H/C and O/C ratios of kerogen mainly ranged from 0.8 to 1.3 and 0.06 to 0.11, respectively, indicating that the kerogen of Jurassic source rocks in the Biloucuo area is type II_1.

The average level of $S_1 + S_2$ within Jurassic source rock samples in the Biloucuo area was 15.0 mg/g of rock, indicating a very high hydrocarbon generation potential. On the

basis of the relationships between the quantity of soluble hydrocarbons in the present strata and the contents of S_2 and TOC, it can be inferred that the hydrocarbon generation conversion rate of these Jurassic source rocks was between 25% and 50%, and a partial hydrocarbon expulsion has taken place. At a greater depth within the study area, the strata of the most significant potential source will reach 20 kg/t of rock, exhibiting particularly good exploration potential.

Author Contributions: Conceptualization, L.X.; methodology, L.X. and Y.S.; software, X.M.; validation, L.X., Y.S. and J.G.; formal analysis, J.G.; investigation, X.M.; resources, Y.S.; data curation, L.X.; writing—original draft preparation, L.X.; writing—review and editing, L.X. and Y.S.; All authors have read and agreed to the published version of the manuscript.

Funding: This research received no external funding.

Conflicts of Interest: The authors declare no conflict of interest.

References

1. Kearney. *Statistical Review of World Energy*, 73rd ed.; Energy Institute: London, UK, 2024.
2. Qin, J.Z. Depositional environment of the marine hydrocarbon source rock in the Qiangtang basin, Qinghai-Tibet plateau. *Pet. Geol. Exp.* **2006**, *28*, 8–14. (In Chinese with English Abstract)
3. Wang, J.; Fu, X.G.; Shen, L.J.; Tan, F.W.; Song, C.Y.; Chen, W.B. Prospect of the potential of oil and gas resources in Qiangtang basin, Xizang (Tibet). *Geol. Rev.* **2020**, *66*, 1091–1113. (In Chinese with English Abstract)
4. Wu, Z.H.; Ji, C.J.; Zhao, Z.; Chen, C. Buried depth evolution and hydrocarbon generation history of the Jurassic system in central Qiangtang Basin. *Acta Geol. Sin.* **2020**, *94*, 2823–2833. (In Chinese with English Abstract)
5. Zhao, G.T.; Li, J.W.; Deng, X.; Cao, Z.Y. Geology characterization and hydrocarbon accumulation pattern of oil sand in Longeni of Qiangtang basin. *Spec. Oil Gas Reserv.* **2019**, *26*, 40–44. (In Chinese with English Abstract)
6. Ding, W.L.; Li, C.; Su, A.G.; He, Z.H. Study on the comprehensive geochemical cross section of Mesozoic marine source rocks and prediction of favorable hydrocarbon generation area in Qingtang basin, Tibet. *Acta Petrol. Sin.* **2011**, *27*, 878–896.
7. Gan, K.W. Evolution and hydrocarbon distribution of Thetysdomain. *Mar. Orig. Pet. Geol.* **2000**, *5*, 21–29.
8. Jia, C.Z.; Yang, S.F.; Chen, H.L.; Wei, G.Q. *Tectonic Geology and Natural Gas in Northern Tethys Basin Group*; Petroleum Industry Press: Beijing, China, 2001.
9. Fu, X.G.; Wang, J.; Tan, F.W.; Chen, M.; Li, Z.X.; Chen, W.B.; Feng, X.L. Recent progress in oil and gas geological exploration in the Qiangtang Basin, Northern Xizang. *Sediment. Geol. Tethyan Geol.* **2015**, *35*, 16–24. (In Chinese with English Abstract)
10. Xu, L.; Luo, S.Q.; Tang, H.; Hu, L.; Xiao, J.; Sun, R.Y. Study on petroleum geological conditions in Dazhuom area of southern Qiangtang basin of Tibet. *Geol. Surv. China* **2020**, *7*, 16–24. (In Chinese with English Abstract)
11. Wang, Z.J.; Wang, J.; Chen, W.X.; Fu, X.G. Discovery of the Late Jurassic Shenglihe marine oil shale in the northern Qiangtang basin, Qinghai-Tibet plateau. *Geol. Bull. China* **2007**, *26*, 764–768.
12. Li, G.J.; Xia, G.Q.; Yi, H.S.; Ji, C.J.; Yang, J.B. Characteristics of the Mesozoic marine argillaceous source rocks and prediction of favorable hydrocarbon generation area in south Qiangtang Depression, Xizang (Tibet). *Geol. Rev.* **2020**, *66*, 1241–1259.
13. Chen, W.B.; Liao, Z.L.; Zhang, Y.J.; Peng, Z.M. Geochemical characteristics and significance of hydrocarbon source rocks in the Jurassic Bi Qu formation in the north Qiangtang basin. *Geol. China* **2007**, *34*, 928–934.
14. Tu, X.X.; Shen, B.; Shi, F.; Wang, S.Q.; Sun, W.L.; Xu, X.M. Determination of residual TOC in special samples-Taking Qiangtang basin as example. *Sci. Technol. Eng.* **2016**, *16*, 110–113.
15. Decelles, P.; Kapp, P.; Ding, L.; Gehrels, G. Late cretaceous to middle tertiary basin evolution in the central Tibetan plat-eau: Changing environments in response to tectonic partitioning, aridification, and regional elevation gain. *Geol. Soc. Am. Bull.* **2007**, *119*, 654–680. [CrossRef]
16. Ding, W.L.; Wan, H.; Zhang, Y.Q.; Han, G.Z. Charaeteristics of the Middle Jurassic marine source rocks and prediction of favor-able source rock kitchens in the Qiangtang basin of Tibet. *J. Asian Earth Sci.* **2013**, *66*, 63–72. [CrossRef]
17. Wu, Z.H.; Gao, R.; Lu, Z.W.; Ye, P.S.; Lu, L.; Yin, C.Y. Structures of the Qiangtang basin and its significance to oil-gas exploration. *Acta Geol. Sin.* **2014**, *88*, 1130–1144. (In Chinese with English Abstract)
18. Ma, A.L.; Hu, X.M.; Garzanti, E.; Han, Z.; Lai, W. Sedimentary and tectonic evolution of the southern Qiangtang basin: Implications for the Lhasa-Qiangtang collision timing. *J. Geophys. Res.-Solid Earth* **2017**, *122*, 4790–4813. [CrossRef]
19. Wang, Z.W.; Wang, J.; Fu, X.G.; Feng, X.L.; Armstrong-Altrin, J.S.; Zhan, W.Z.; Wan, Y.L.; Song, C.Y.; Ma, L.; Shen, L.J. Sedimentary auccessions and onset of the Mesozoic Qiangtang rift basin (northern Tibet), southwest China: Insights on the Palaeo and Meso-tethys evolution. *Mar. Petrol. Geol* **2019**, *102*, 657–679. [CrossRef]

20. Huang, D.F.; Li, J.C.; Gu, X.Z. *Evolution and Hydrocarbon Generating Mechanism of Terrigenous Organic Matter*; Petroleum Industry Press: Beijing, China, 1984.
21. Gao, G.; Xian, B.L.; Ren, J.L.; Zhang, W.W.; Ma, W.Y. Origin and source of natural gas from Wuxia fault belt in northern Mahu sag, Junggar basin. *Nat. Gas Geosci.* **2016**, *27*, 672–681.
22. Chen, J.P.; Liang, D.G.; Zhang, S.C.; Deng, C.P.; Zhao, Z.; Zhang, D.J. Evaluation criterion and methods of the hydrocarbon generation potential for China's paleozoic marine source rocks. *Acta Geol. Sin.* **2012**, *86*, 1132–1142. (In Chinese with English Abstract)
23. Tissot, B.P.; Welte, D.H. *Petroleum Fomation and Occurrence*; Springer: Berlin/Heidelberg, Germany, 1994.
24. Chen, W.B.; Liao, Z.L.; Liu, J.Q.; Fu, X.G.; Du, B.W.; Feng, X.L.; Du, Q.D. Geochemistry of the Jurassic source rocks in the south Qiangtang basin, Tibet. *Geoscience* **2010**, *24*, 654–661. (In Chinese with English Abstract)
25. Fu, X.G.; Wang, J.; Wang, Z.J.; He, J.L. Characteristics of kerogens and their carbon isotope implications for the Shengli river oil shale in Qiangtang basin, northern Tibet. *Acta Geosci. Sin.* **2009**, *30*, 643–650. (In Chinese with English Abstract)
26. Cornford, C. *Organic Petrography of Lower Cretaceous Shales at DSDP Leg4 Site 398, Vigo Seamount, Eastern North Atlantic*; Texas A & M University, Ocean Drilling Program: College Station, TX, USA, 1979; Volume 47, pp. 523–527.
27. Xu, L.; Shi, Y.J.; Chen, X.D.; Wan, C.Z.; Wang, J.G. Kinetic analysis of hydrocarbon generation based on saline lacustrine source rock and kerogen in the western Qaidam Basin, China. *Carbonates Evaporites* **2018**, *34*, 1045–1053. [CrossRef]
28. Hugher, W.B.; Holba, A.G.; Dzou, L.I.P. The ratios of dibenzothiophene to phenanthrene and pristane to phytane as indicators of depositional environment and lithology of petroleum source rocks. *Geochim. Cosmochim. Acta* **1995**, *43*, 739–745.
29. Koopmans, M.P.; Rijpstra, W.I.; Klapwijk, M.M.; Leeuw, J.W.; Lewan, M.D.; Sinninghe Damste, J.S. A thermal and chemical degradation approach to decipher pristane and phytane precursors in sedimentary organic matter. *Org. Geochem.* **1999**, *30*, 1089–1104. [CrossRef]
30. Ten Haven, H.L.; De Leeum, J.W.; Rullkotter, J. Restricted utility of the pristine/phytane ratio as a paleoenvironmental indicator. *Nature* **1987**, *330*, 641–643. [CrossRef]
31. Moldowan, J.M.; Sundararaman, P.; Schoell, M. Sensitivity of biomarker properties to depositional environment and/or source input in the lower tocrcian of SW-Germany. *Org. Geochem.* **1986**, *10*, 915–926. [CrossRef]
32. Peters, K.E.; Moldowan, J.M. *The Biomarker Guide: Interpreting Molecular Fossils in Petroleum and Ancient Sediment*; Prentice-Hall: Englewood Cliffs, NJ, USA, 1993.
33. Pan, C.C.; Peng, D.H.; Zhang, M.; Yu, L.P.; Sheng, G.Y.; Fu, J.M. Distribution and isomerization of C_{31}-C_{35} homohopanes and C_{29} steranes in oligocene saline lacustrine sediments from Qaidam Basin, Northwest China. *Org. Geochem.* **2008**, *39*, 646–657. [CrossRef]
34. Fu, J.M.; Sheng, G.Y. Source and biomarker composition characteristics of Chinese non-marine crude oils. *Acta Sedimentol. Sin.* **1991**, *9*, 1–8.
35. Duan, Y.; Wang, C.Y.; Zheng, C.Y. Geochemical study of crude oils from the Xifeng oilfield of the Ordos Basin, China. *J. Asian Earth Sci.* **2008**, *31*, 341–356. [CrossRef]
36. Cheng, K.M. *Oil and Gas Generation of Tuha Basin*; Petroleum Industry Press: Beijing, China, 1994.
37. Wu, Y.J.; Wang, S.; He, L.; Wang, Z.D.; Nie, Z.Q. Research on the burial history and the thermal evolution history of the Jurassic coal-measure source rocks in the eastern margin of Xiaocaohu Sag. *Northwestern Geology.* **2021**, *54*, 180–191. (In Chinese with English Abstract)